A Criterion for Ductile Fracture by the Growth of Holes

F. A. McCLINTOCK
Professor of Mechanical Engineering,
Massachusetts Institute of Technology,
Cambridge, Mass.

From an available solution for the deformation of elliptical holes in a viscous material, a criterion is developed for fracture by the growth and coalescence of cylindrical holes under any prescribed history of applied principal components of stress and strain which do not rotate relative to the material. The criterion is extended to plastic materials by extrapolation from an analysis for the growth of circular holes under equiaxial transverse stress. Experiments on Plasticine substantiate the analysis and its extrapolation. For both plastic and viscous flow, most of the applied strain to fracture is found to occur while the holes are still small compared with their spacing. The most striking result is that in plastic materials there is a very strong inverse dependence of fracture strain on hydrostatic tension. The theory also indicates the effects of anisotropy, strain-hardening, and strain gradients on ductile fracture by the growth of holes.

Introduction

FRACTURE by the growth of holes has been observed in ductile metals by Tipper [1],[1] Plateau, Henry, and Crussard [2], Puttick [3], Rogers [4], and Bluhm and Morrissey [5]. Rhines [6] has shown marked similarities between the growth of voids in Plasticine and those observed in copper by Puttick (see Fig. 1). Furthermore, using polystyrene spheres as "inclusions" in his Plasticine, he was able to develop and suppress "wolf's ear" fractures similar to those Backofen [7] found in copper under torsion followed by tension (see Fig. 2). Rhines found that very high inclusion densities were required for fracture in Plasticine, perhaps because the inclusions tended to adhere to the matrix. He also found that notch sensitivity and reduction of area were size-dependent.

These similarities to fracture in metals suggest that where the inclusions are large enough to be observed under the microscope, fracture by the growth of holes can be considered to be primarily a problem in continuum mechanics. Recent studies of the mechanism of hole growth [8–10] have been largely empirical, have considered cases where the holes interact from the beginning, and have neglected triaxiality as a variable. As a complement to these studies, a more theoretical analysis seems in order.

Representation of Criteria for Fracture by Hole Growth

Before turning to detailed but still approximate calculations, it is worth examining the attributes which any criterion for ductile fracture by the growth of holes must have. Criteria for initial yielding or for brittle fracture require only the current state of stress. In ductile fracture by the growth of holes, however, the changes in the size, shape, and spacing of the holes will depend on the entire history of stress, strain, and rotation. This added complexity is probably typical of ductile fracture in general, and may be part of the reason for the current absence of ductile fracture criteria. It is this absence which makes it worthwhile to study even the simple models which will be considered here.

To simplify its representation, the history will be restricted to cases in which the principal components of stress do not rotate relative to the material, although they may vary in magnitude.

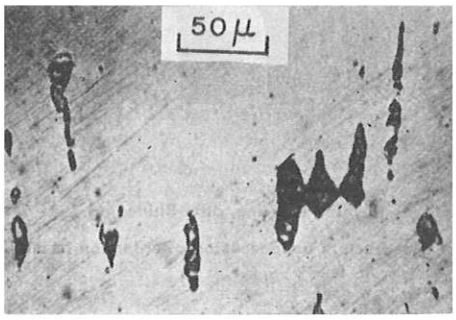

(a) in copper, after Puttick [3]

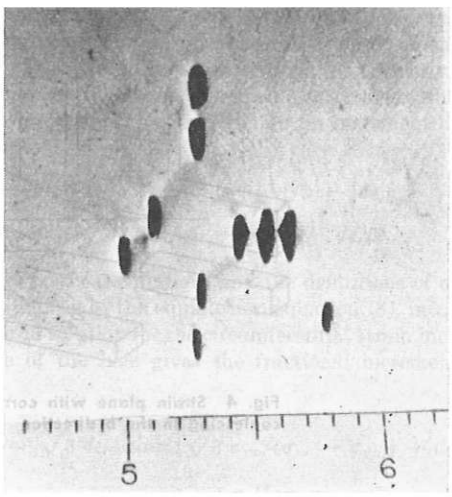

(b) in Plasticine, after Rhines [6]

Fig. 1 Coalescence of holes

In other words, we shall consider the normal and the delamination types of fracture shown in Fig. 3 from Bluhm and Morrissey [11], but not the incipient fracture in the shear band, which is discussed elsewhere [12]. Thus only the principal components of stress and strain need be considered. Since the holes turn out to be relatively small over most of the life of the specimen, the components of applied stress and strain will be related by the usual stress-strain relations for an incompressible, fully plastic material, reducing the number of independent variables to three. I propose the most symmetrical representation, which uses the fact that the sum of the three normal strain components is zero, so that the strain can be represented in triangular coordinates on a plane. The one independent component of stress may be taken to be the ratio of the mean normal stress to the equivalent flow

[1] Numbers in brackets designate References at end of paper.

Contributed by the Applied Mechanics Division and presented at the Applied Mechanics Conference, Providence, R. I., June 12–14, 1968, of THE AMERICAN SOCIETY OF MECHANICAL ENGINEERS.

Discussion of this paper should be addressed to the Editorial Department, ASME, United Engineering Center, 345 East 47th Street, New York, N. Y. 10017, and will be accepted until July 15, 1968. Discussion received after the closing date will be returned. Manuscript received by the ASME Applied Mechanics Division, December 26, 1967. Paper No. 68—APM-14.

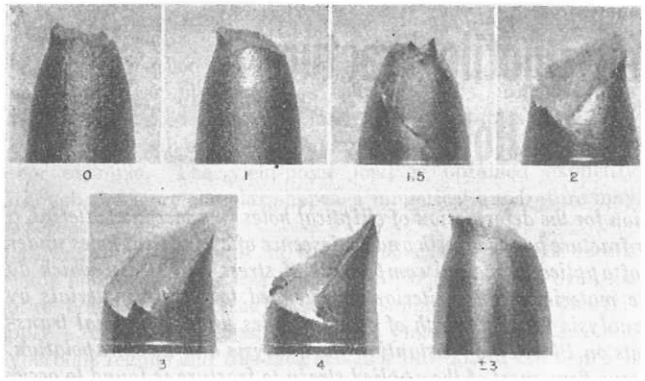

(a) in copper, after Backofen, et al. [7]

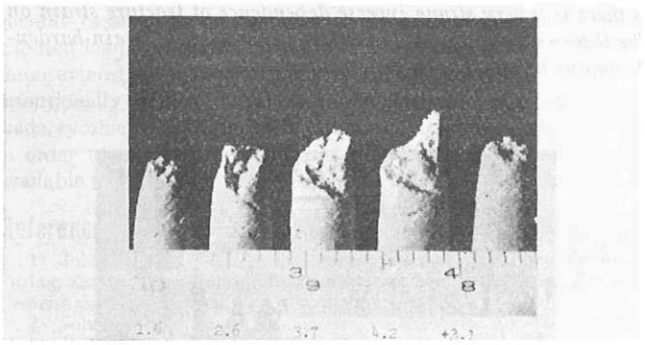

(b) in Plasticine, after Rhines [6]

Fig. 2 Wolf's ear fracture under tension after torsion to indicated shear strains

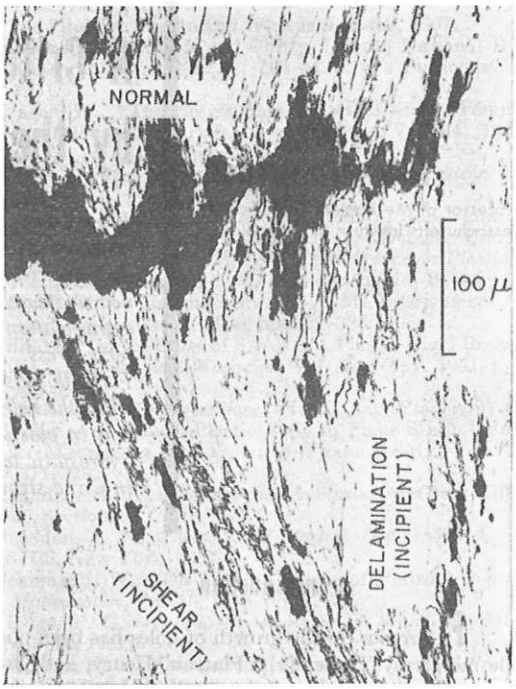

Fig. 3 Growing normal fracture and incipient delaminating and shear fractures in necked copper tensile specimen, U. S. Army Materials Research Agency [11]

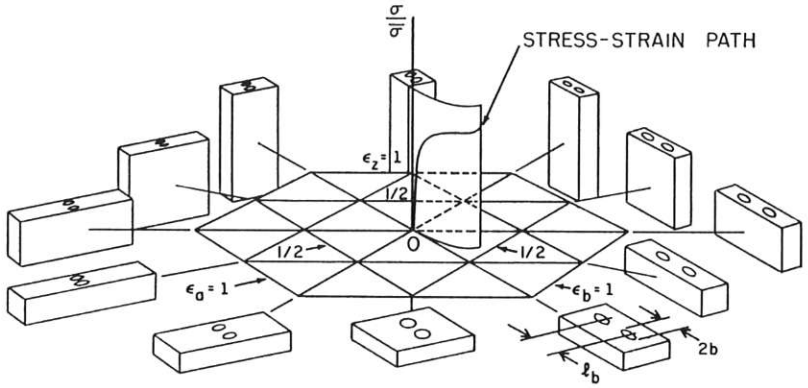

Fig. 4 Strain plane with corresponding deformations of a cube containing z holes coalescing in the b direction

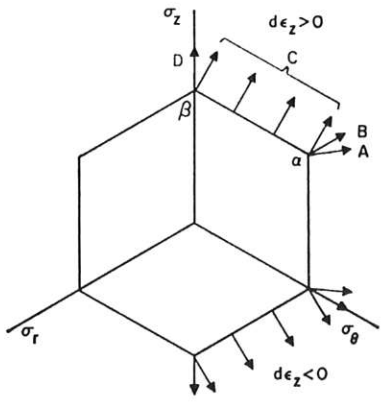

Fig. 5 Stress determined from strain increments and associated Tresca flow rule around a hole with radial and axial strain

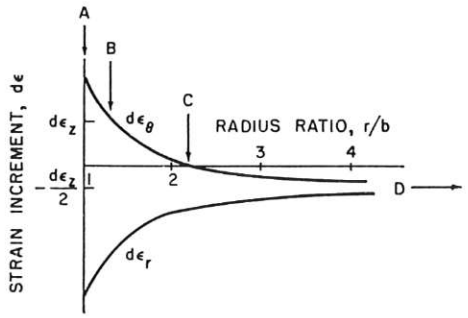

Fig. 6 Strain distribution around a hole under radial and axial strain

stress of the material. Such coordinates are shown in Fig. 4, along with the final shapes of an initially cubic element deformed along various radial paths. The Cartesian coordinates are labeled a, b, and z to correspond to the major, minor, and axial directions of elliptical holes to be considered below.

For any given increment in principal strain, the corresponding components of stress can be determined from the stress-strain relations. For the Mises yield criterion and associated flow rule, in terms of the mean normal stress, σ, and the equivalent stress and strain, $\bar{\sigma}$ and $d\bar{\epsilon}$:

$$d\epsilon_1 = 3(\sigma_1 - \sigma)d\bar{\epsilon}/2\bar{\sigma}$$

or

$$\sigma_1/\bar{\sigma} = \sigma/\bar{\sigma} + 2d\epsilon_1/3d\bar{\epsilon}, \quad (1)$$

$$\sigma_2/\bar{\sigma} \text{ and } \sigma_3/\bar{\sigma} \text{ similarly.}$$

For the maximum shear stress or Tresca yield criterion, the stress for a given strain increment may be found from a sketch of the yield locus. For convenience, define $d\epsilon_1$, $d\epsilon_2$, and $d\epsilon_3$ as the maximum, intermediate, and minimum principal strain increments, respectively. Then, except when $d\epsilon_2 = 0$, one is at the corners of the yield locus and from the associated flow rule,

$$\text{for } d\epsilon_2 > 0, \quad \sigma_1 - \sigma_3 = \sigma_2 - \sigma_3 = 2k,$$

or (2)

$$\text{for } d\epsilon_2 < 0 \quad \sigma_1 - \sigma_2 = \sigma_1 - \sigma_3 = 2k,$$

where k is the yield strength in shear.

From the stress differences and the mean normal stress, the principal components of stress can be found. For example:

$$\sigma_1 = \sigma + (\sigma_1 - \sigma_2 + \sigma_1 - \sigma_3)/3. \quad (3)$$

Thus for each increment of a stress and strain path through the three-dimensional space of Fig. 4, all six principal components of applied stress and strain can be determined. These components, in turn, will determine the deformation of the holes, which eventually leads to fracture.

A diagram such as Fig. 4 is also useful for other mechanisms of fracture under plastic flow. For example, it can be used to describe the path of an element in low-cycle fatigue under complex stress-strain histories where the hysteresis loop is not a plane figure involving just one component of stress or one of strain.

Analysis

General assumptions. The material is assumed to contain three mutually perpendicular sets of cylindrical holes of elliptical cross-section with axes parallel to the principal directions of the applied stress (and strain increment). One such family is shown in Fig. 4. Each hole is considered surrounded by a cylindrical cell whose dimensions are of the order of the mean spacing between the holes. It will be assumed that most of the applied strain occurs while the holes are still small enough so that their interactions with each other may be neglected. The mechanics problem then reduces to the generalized plane-strain deformation of a hole in an infinite medium. The hole may lengthen or shorten and will continue to have a more or less elliptical cross section. The condition of fracture will be that the growth of the holes (calculated as if they were in an infinite medium) is such that each hole touches a pair of its cell walls. In other words, one of the semiaxes a or b of the hole approaches half the corresponding cell size (mean spacing), $l_a/2$ or $l_b/2$, respectively. This condition may be described in terms of a relative growth factor giving the increase in semiaxis of the hole relative to the corresponding hole spacing. For instance, for holes with a cylindrical axis in the z direction, growing in the b direction as shown in Fig. 4, the relative growth factor is defined as

$$F_{zb} = (b/l_b)/(b^0/l_b{}^0). \quad (4)$$

There are, in general, six possible modes of fracture; holes with a z axis in any one of the three directions can coalesce in either of two transverse directions. For instance, the relative hole growth factor at fracture due to z holes growing together in the b direction is

$$F_{zb}{}^f = (1/2)/(b^0/l_b{}^0). \quad (5)$$

Because of prior mechanical history, the initial semiaxes and spacings may be different in different directions. Thus for the specimen as a whole, fracture occurs on the ij plane (holes parallel to the x_i axis coalesce in the j direction) when the ij growth factor is the first to reach its critical value for fracture:

$$F_{ij} = F_{ij}{}^f. \quad (6)$$

For tests with a varying stress history, it is convenient to have a measure of damage which is additive and accumulates to unity at fracture. This is obtained by defining the damage as

$$d\eta_{ij} = d(\ln F_{ij})/\ln F_{ij}{}^f. \quad (7)$$

Circular holes in a Mises material. Solutions for the growth of holes in a plastic material are in general known only for circular holes under axisymmetric applied stress and either plane stress or plane strain. The solution for generalized plane strain is developed here for a nonstrain-hardening material. In this plastic analysis the applied stress will be denoted by the subscript (∞) (e.g., $\sigma_{r\infty}$), to distinguish it from the local stress (σ_r). Elsewhere in the paper the subscript will be dropped for simplicity. The radial stress for a given increment of hole growth is found by starting with the equilibrium equation,

$$\partial\sigma_r/\partial r + (\sigma_r - \sigma_\theta)/r = 0, \quad (8)$$

and expressing the stress difference in terms of the strain difference from the stress-strain relations, equation (1),

$$\partial\sigma_r/\partial r = -(2\bar{\sigma}/3r)(d\epsilon_r/d\bar{\epsilon} - d\epsilon_\theta/d\bar{\epsilon}). \quad (9)$$

The strain increments are found by integrating the strain-displacement equations along with the condition of incompressibility, which yields the following equations for the distribution of radial and tangential strain increments in terms of the uniform axial strain increment, $d\epsilon_z$, and the strain increment $d\epsilon_{\theta b}$ at the inner radius, b:

$$\begin{aligned} d\epsilon_r &= -(b^2/r^2)(d\epsilon_{\theta b} + d\epsilon_z/2) - d\epsilon_z/2, \\ d\epsilon_\theta &= (b^2/r^2)(d\epsilon_{\theta b} + d\epsilon_z/2) - d\epsilon_z/2. \end{aligned} \quad (10)$$

Substitution of these equations and the definitions of equivalent stress and strain into the equilibrium equation (8), integration of the result, and solution for the circumferential strain increment at the surface of the hole gives the fractional increment in hole diameter:

$$d\ln(b/b^0) = \sqrt{3}\, d\epsilon_{r\infty} \sinh\left[\sqrt{3}\,\sigma_{r\infty}/(\sigma_{r\infty} - \sigma_{z\infty})\right] + d\epsilon_{r\infty}. \quad (11)$$

Circular holes in a Tresca material. Here piecewise integration is needed for the different regimes of the yield locus of Fig. 5. For increases in the ratio of hole diameter to spacing, the circumferential strain at the surface of the hole and the axial strain must be related so that

$$d\ln(b/l) = db/b - dl/l = d\epsilon_{\theta b} + d\epsilon_z/2 > 0,$$

or from incompressibility,

$$d\epsilon_{\theta b} > d\epsilon_{rb}. \quad (12)$$

This limits the strain increments and stress to the right half of Fig. 5. The strain increments depend only on symmetry, incompressibility, and compatibility and are again given by equations (10) as shown in Fig. 6. From the associated Tresca flow rule, the states of stress must lie along the parts of the yield locus indicated in Fig. 5. For $d\epsilon_z > 0$, the tangential strain increment vanishes at the critical radius found from equations (10) to be

$$r_C/b = \sqrt{1 + 2d\epsilon_{\theta b}/d\epsilon_z}. \tag{13}$$

At larger radii, the circumferential strain becomes negative, and the state of stress is confined to the vertex β of Fig. 5, so that $\sigma_\theta = \sigma_r$. From the equilibrium equation, there will be no further change in radial stress. The applied stress $\sigma_{r\infty}$ is thus found by integrating equation (8) from b to r_C with $\sigma_\theta - \sigma_r = 2k$. The resulting equation is solved for the increment in radius of the hole. The hole growth for $d\epsilon_z < 0$ is found similarly:

for $d\epsilon_z > 0$ (i.e., $d\epsilon_{r\infty} < 0$),

$$d \ln (b/b^0) = -d\epsilon_{r\infty} \exp [-2\sigma_{r\infty}/(\sigma_{r\infty} - \sigma_{z\infty})] + d\epsilon_{r\infty},$$

for $d\epsilon_z < 0$ (i.e., $d\epsilon_{r\infty} > 0$), (14)

$$d \ln (b/b^0) = -d\epsilon_{r\infty} \exp [2\sigma_{r\infty}/(\sigma_{r\infty} - \sigma_{z\infty})] + d\epsilon_{r\infty}.$$

Comparison of equations (14) with equation (11) for the Mises material indicates a similar exponential dependence on radial stress for high values of transverse stress. For convenience, only the Mises material will be considered from here on.

Elliptical holes on a viscous material. The only plastic solution for holes without circular symmetry is that of Drucker [13], who showed that, for plane-strain distortion of a cylindrical hole in a nonhardening plastic material, the strain should be confined to shear planes running from the hole either to a free surface or to a neighboring hole. This would lead to thin layers of highly strained material adjacent to unstrained material. Such a strain concentration would be diffused by a small amount of strain hardening. A better boundary condition would be to impose uniform strain at large distances from the hole, but this solution is not known. Another possibility is a viscous solution, which allows the effects of strain history and the permanence of the deformation to appear, and diffuses the high strain concentrations. It has the disadvantage that the "hardness" depends on the strain rate and not on the previous history of plastic straining. Nonetheless, the viscous and nonhardening materials seem to provide limiting cases between which the behavior of moderately strain-hardening materials is likely to lie [14]. We therefore turn to the viscous case, for which solutions exist.

Berg [15] gave the change in shape of an elliptical hole in terms of the mean radius, R, and the eccentricity, m, defined in terms of the semimajor and semiminor axes a and b as

$$R = (a + b)/2, \qquad m = (a - b)/(a + b). \tag{15}$$

For plane strain with constant applied stress in the principal directions σ_a and σ_b (dropping the subscript ∞), his equations (21) and (22a) give the change in size and shape of the holes in terms of the time t and the coefficient of viscosity μ:

$$\ln R/R^0 = (\sigma_a + \sigma_b)t/4\mu, \tag{16}$$

$$m = \frac{\sigma_a - \sigma_b}{\sigma_a + \sigma_b} + \left(m^0 - \frac{\sigma_a - \sigma_b}{\sigma_a + \sigma_b}\right) \exp\left[-\frac{(\sigma_a + \sigma_b)t}{2\mu}\right]. \tag{17}$$

For comparison with plasticity, the time and viscosity can be expressed in terms of the equivalent strain by introducing the definition

$$\bar{\epsilon} = \left[\frac{2}{9}\left[(\epsilon_a - \epsilon_b)^2 + (\epsilon_b - \epsilon_z)^2 + (\epsilon_z - \epsilon_a)^2\right]\right]^{1/2},$$

where

$$\epsilon_a = \left[\sigma_a - \frac{1}{2}(\sigma_b + \sigma_z)\right]t/3\mu, \tag{18}$$

and similarly for ϵ_b and ϵ_z, giving

$$t/\mu = 3\bar{\epsilon}/\bar{\sigma}.$$

Solutions for generalized plane strain can be found for linearly viscous materials by superimposing a uniaxial stress parallel to the axis of the hole, which changes the size of the hole by the factor $\exp(-\epsilon_z/2)$ but leaves the shape unaffected. Combination of these steps leads to expressions which will be put in terms of the transverse stress components and $(\epsilon_a + \epsilon_b)/2$ for later convenience:

$$\ln R/R^0 = 3\bar{\epsilon}(\sigma_a + \sigma_b)/4\bar{\sigma} + (\epsilon_a + \epsilon_b)/2, \tag{19}$$

$$m = \frac{\sigma_a - \sigma_b}{\sigma_a + \sigma_b} + \left(m^0 - \frac{\sigma_a - \sigma_b}{\sigma_a + \sigma_b}\right) \exp\left[-\frac{3}{2}\frac{(\sigma_a + \sigma_b)}{\bar{\sigma}}\bar{\epsilon}\right]. \tag{20}$$

Extrapolation to elliptical holes in a plastic material. Pending exact solutions for elliptical holes in a plastic material, it is worth estimating the behavior from that of the viscous material. For the special case of circular holes under axisymmetrical applied stress, direct solution of the equilibrium equation (8), the strain-displacement equations (10), and the viscous stress-strain relation gives

$$\ln b/b^0 = 3\epsilon_r\sigma_r/(\sigma_r - \sigma_z) + \epsilon_r. \tag{21}$$

For the mean radius R, the expression for the viscous circular case is transformed into the elliptical one by the substitutions in the first term

$$\epsilon_r \to \bar{\epsilon}/2, \qquad \sigma_r \to (\sigma_a + \sigma_b)/2, \quad \text{and} \quad (\sigma_r - \sigma_z) \to \bar{\sigma},$$

and in the second term

$$\epsilon_r \to (\epsilon_a + \epsilon_b)/2.$$

While the form used here for the plastic equation (11) suggests a similar substitution, the form was not immediately obvious, and a review of the conditions on the substitution is in order. If one substituted $[(\sigma_a + \sigma_b)/2] - \sigma_z$, rather than $\bar{\sigma}$, for $\sigma_r - \sigma_z$, then an infinity would arise in the limiting case of plane strain, $\sigma_z = (\sigma_a + \sigma_b)/2$. This infinity does not appear in the viscous case because ϵ_r goes to zero as rapidly as $\sigma_r - \sigma_z$ in equation (21). With the hyperbolic sine of equation (11), however, these zeros are of different orders of magnitude. Likewise, the introduction of $\bar{\epsilon}/2$ for ϵ_r is suggested by the fact that, without it, under plane strain conditions ($\epsilon_a = -\epsilon_b$), there would be no change in the mean radius no matter what the applied radial stress. The substitution of $(\epsilon_a + \epsilon_b)/2$ rather than $\bar{\epsilon}/2$ for ϵ_r in the second term is made because, if $\bar{\epsilon}/2$ were used, the resulting expression would not reduce to the viscous case for small values of the argument of the hyperbolic sine even for circular holes, as it must according to equations (11) and (21).

At the same time these changes are introduced, it is well to account for the possibility of strain hardening. McClintock and Rhee [14] have shown that in many cases this can be done approximately with the aid of the hardening coefficient, n, appearing in $\sigma = \sigma_1\epsilon^{-n}$ or alternatively defined in terms of the stress at the point of maximum strain divided by the average stress over the stress-strain curve up to the maximum strain:[2]

$$n = [(\bar{\sigma}_{\text{at max}}\ \bar{\epsilon})/(\bar{\sigma}_{\text{avg to max}}\ \bar{\epsilon})] - 1. \tag{22}$$

This strain-hardening coefficient ranges from zero for a nonhardening material to unity for a linearly hardening material. Incorporating this coefficient as an interpolator for the changes discussed above leads to the following expression for the mean radius of elliptical holes in a plastic material:

$$\ln R/R^0 = \frac{\bar{\epsilon}\sqrt{3}}{2(1 - n)} \sinh\left(\frac{\sqrt{3}\ (1 - n)}{2}\frac{(\sigma_a + \sigma_b)}{\bar{\sigma}} + \frac{\epsilon_a + \epsilon_b}{2}\right). \tag{23}$$

The eccentricity m might have a different steady-state value

[2] Where the applied strain at infinity is relatively large, it appears better to take the average stress up to the maximum local equivalent strain starting from the applied equivalent strain rather than from zero.

and a different rate of approach to it. Tentatively, let the steady-state rate be the same as for a viscous material, and let the argument of the exponential transform as does the first term from equation (19) to equation (23):

$$m = \frac{\sigma_a - \sigma_b}{\sigma_a + \sigma_b} + \left(m^0 - \frac{\sigma_a - \sigma_b}{\sigma_a + \sigma_b}\right) \times \exp\left[-\frac{\sqrt{3}\,\bar{\epsilon}}{(1-n)} \sinh\left(\frac{\sqrt{3}\,(1-n)}{2}\,\frac{\sigma_a + \sigma_b}{\bar{\sigma}}\right)\right]. \quad (24)$$

Before applying equations (23) and (24) to ductile fracture, experimental evidence will be given for their validity. Plasticine was used instead of a metal to obtain the required large strains around the holes without local fracture and with little strain hardening. It also simplified the experimental procedure. A typical stress-strain curve is shown in Fig. 7. Application of equation (22) for an equivalent strain of 0.5 gives a strain-hardening index of about 0.35. Hybels [16] ran experiments with equal biaxial tension using a bulge test, and East [17] ran experiments on bending in plane strain and plane stress. The corresponding transverse and axial stress ratios in the three cases were, respectively, 1:1:0, 1.155:0.577:0, and 1:0:0. The equivalent strain was determined from gage marks initially six or more hole diameters apart.

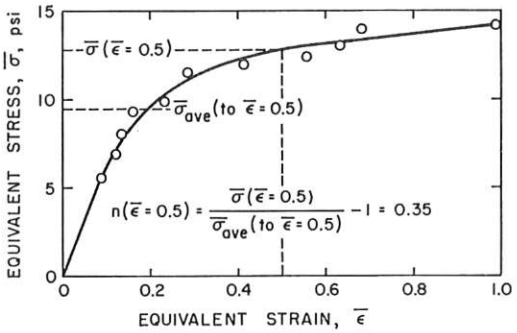

Fig. 7 Compressive stress-strain curve for Plasticine

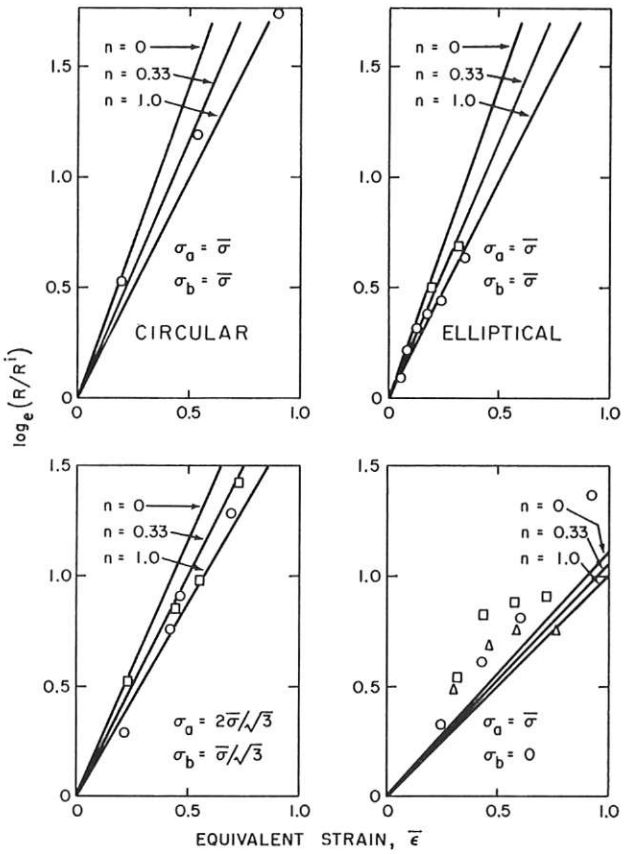

Fig. 8 Growth of mean radius as a function of strain in Plasticine. Different symbols indicate different specimens

The results for the mean radius ratio are shown in Fig. 8, along with the theoretical predictions for various strain-hardening coefficients n. The rate of hole growth predicted by equation (23) for plastic materials ($n < 1$) is not inconsistent with the data, and may even be exceeded for the uniaxial case, $\sigma_a = \bar{\sigma}$, $\sigma_b = 0$.

Similar results for eccentricity are shown in Fig. 9 for two or three specimens at each stress ratio. The theoretical steady-state eccentricity is perhaps 25 percent low in one case and 10 percent high in another. The rate of approach to the steady-state value seems good in two cases and perhaps low by a factor of two in the third. Since there is no regular pattern and since eccentricity turns out to have a small effect in the fracture criterion, it is sufficient to estimate its order of magnitude from equation (24).

With this experimental evidence, we return to the analysis for the fracture criterion using equation (23) for the radius ratio and equation (24) for the eccentricity.

Fracture criterion for constant stress ratios. The relative hole growth factor F involves the semiaxis b of the hole, which can be obtained from equations (23) and (24) along with equations (15) defining R and m, and the hole spacing l_b as determined from the strain at infinity:

$$l_b = l_b^0 \exp \epsilon_b. \quad (25)$$

Hence

$$F_{zb} = \frac{R}{R^0}\,\frac{(1-m)}{(1-m^0)}\,e^{-\epsilon_b}; \quad F_{za} = \frac{R}{R^0}\,\frac{(1+m)}{(1+m^0)}\,e^{-\epsilon_a}. \quad (26)$$

As an example, the growth factor is plotted in Fig. 10 for a viscous material ($n = 1$) with initially round holes ($m^0 = 0$) under applied stress components in the ratio 2:1:0 (encountered in plane-

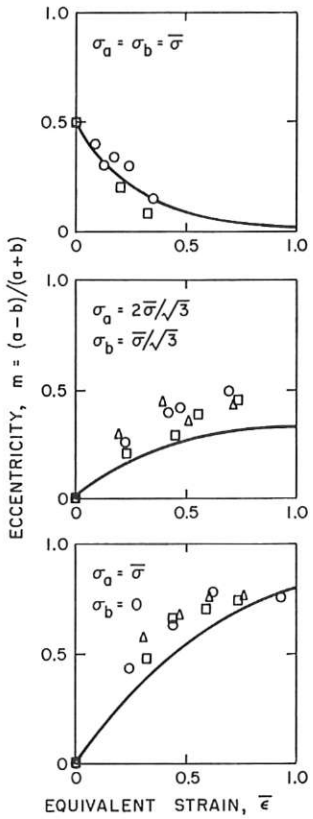

Fig. 9 Shape changes for holes in Plasticine. Solid line from equation (24) for $n = 0.35$. Different symbols indicate different specimens

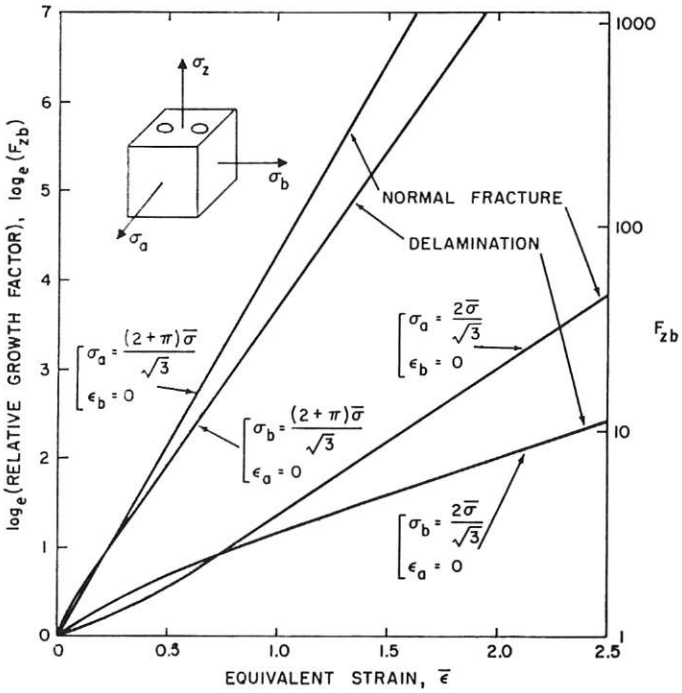

Fig. 10 Relative growth factors for viscous material ($n = 1$). Stress ratios $(2 + \pi):(1 + \pi):\pi$ and 2:1:0, with σ_z the minimum principal stress

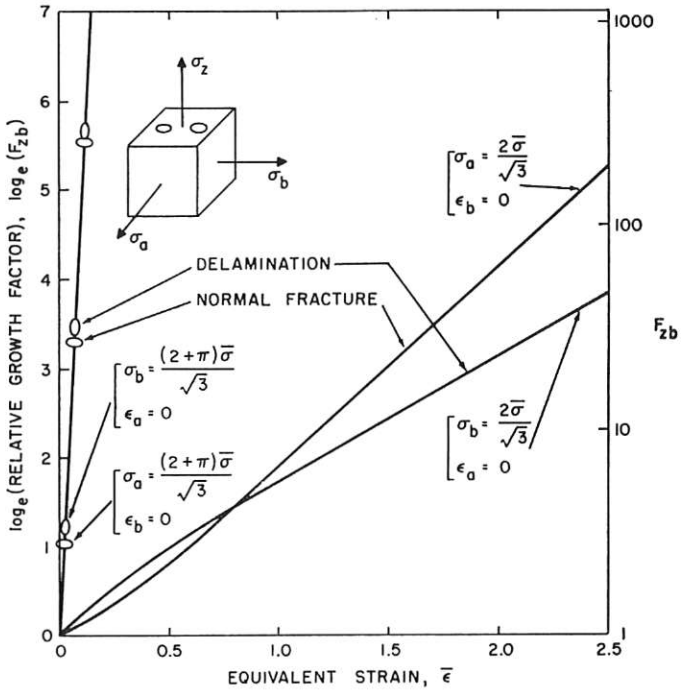

Fig. 11 Relative growth factors for plastic material ($n = 0$). Stress ratios $(2 + \pi):(1 + \pi):\pi$ and 2:1:0, with σ_z the minimum principal stress

strain bending), and $(2 + \pi):(1 + \pi):\pi$ (the maximum expected in a plane strain, doubly grooved, nonhardening tensile specimen). For most rapid growth, σ_a or σ_b is the maximum principal stress, with σ_z the minimum principal stress. Fig. 11 presents the corresponding information for a nonstrain-hardening material ($n = 0$).

The most important observation from Figs. 10 and 11 is the very strong effect of triaxiality in reducing the fracture strain, especially in the nonhardening material.

A second observation from Figs. 10 and 11 is that for "dirty" materials with low growth factors due to a close inclusion spacing, there is a tendency for cracks to open on planes parallel, rather than normal, to the maximum component of applied stress, since $F_{za} > F_{zb}$. This tendency is strong enough at high triaxiality in nonhardening materials so that normal fracture does not occur for the range of growth factors considered here.

A third observation from Figs. 10 and 11 is that the initial transient in damage rate, associated with the change in shape of the holes, dies out relatively quickly. This is expected because most of the contribution to the growth factor F must come from the radius ratio R/R^0, when $R/R^0 \gg 1$, since the eccentricity is never more than unity.

Fracture criterion for varying stress ratios. If the stress history is varying, transients will be repeatedly introduced and should be taken into account. While differential expressions can be obtained, numerical integration is still necessary, so it is just as well to apply equations (23), (24), and (26) for short elements of the path over which the stress ratios are assumed constant. A computer program in MAD language is available on request [18].

Approximate fracture criterion. A closed-form expression for a fracture criterion can be obtained by neglecting transient effects. From equation (26) for the growth factor, equation (23) for the radius ratio, and equation (18) for the stress-strain relation, combined with equation (7) for the definition of damage:

$$\frac{d\eta_{zb}}{d\bar{\epsilon}} = \frac{1}{\ln F_{zb}^{f}}\left[\frac{\sqrt{3}}{2(1-n)}\sinh\left(\frac{\sqrt{3}\,(1-n)}{2}\,\frac{(\sigma_a+\sigma_b)}{\bar{\sigma}}\right) + \frac{3}{4}\,\frac{\sigma_a-\sigma_b}{\bar{\sigma}}\right] \quad (27)$$

The resulting relation is shown in Fig. 12. For nonhardening

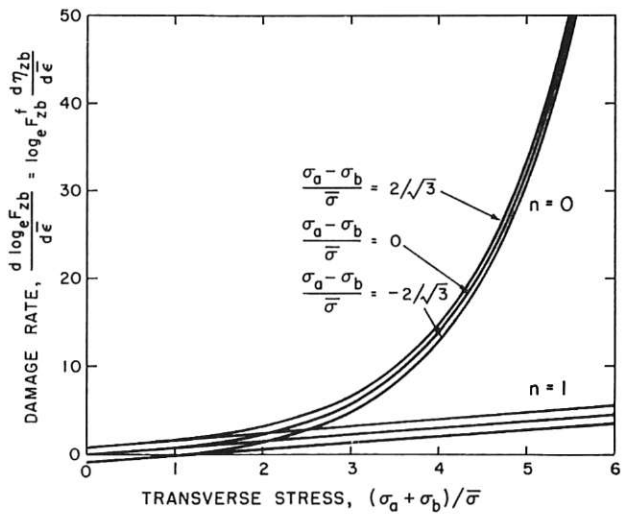

Fig. 12 Steady-state damage rate from equation (27)

materials ($n = 0$), the damage rate tends to depend on the average of the two transverse stresses, whereas for viscous materials it depends only on the stress normal to the fracture plane.

An even simpler expression is desirable, and can be obtained from equation (27) by dropping the last term and expressing the equivalent stress as that found in plane tension:

$$\frac{d\eta_{zb}}{d\bar{\epsilon}} = \frac{\sinh\left[(1-n)(\sigma_a+\sigma_b)/(2\bar{\sigma}/\sqrt{3})\right]}{(1-n)\ln F_{zb}^{f}}. \quad (28)$$

To remember this equation, bear in mind that the damage rate varies as the hyperbolic sine of the sum of the transverse components of applied stress. The factor $1 - n$ appears in such a way that as the strain hardening exponent n goes to unity, the hyperbolic sine approaches its argument and the factor $(1 - n)$ cancels that in the denominator. At the same time the dependence on transverse stress is much reduced.

For constant ratios between components of applied stress, equation (28) can be integrated and combined with equation (5) to obtain the fracture strain required for z-axis holes, with initial

spacing l_b, to coalesce in the b direction:

$$\bar{\epsilon}^f = \frac{(1-n)\ln(l_b^0/2b^0)}{\sinh[(1-n)(\sigma_a+\sigma_b)/(2\bar{\sigma}/\sqrt{3})]}. \quad (29)$$

This expression is good to 15 percent at high triaxiality. At low triaxality it may differ from equation (27) by a factor of two if the transverse stress components are quite unequal.

Discussion

Principal results. The most important implication of equation (27) is the strong inverse dependence of fracture strain on transverse stress. For example, consider a nonstrain-hardening material with a typical volume fraction of inclusions (equal to the area fraction in a random metallographic section) of 10^{-3} to 10^{-4}. The relative hole growth factor is the reciprocal of the ratio $2b^0/l_b^0$, which for uniform spherical inclusions is of the order of the cube root of the void fraction, giving values of F^f of 10 to 20. In plane strain bending, Fig. 11 indicates a fracture strain of 1.2 to 1.5. Under a triaxiality of a doubly grooved, plane strain tensile test, however, the fracture strain would be reduced to 0.05 to 0.06! This low ductility under high triaxiality explains why it is so difficult to study the details of plane strain crack growth: the fully plastic stress and strain distributions are not likely to be attained before local fracture. On the other hand, for low values of transverse stress, the possibility of fracture is governed by the requirements that the holes remain open and the steady state damage rate be positive. The second requirement can be found from the limiting form of equation (27) as the sum of the two transverse stress components goes to zero. The hyperbolic sine then approaches its argument, giving

$$\frac{d\eta_{zb}}{d\bar{\epsilon}} = \frac{1}{\ln F_{zb}^f}\,\frac{3}{4}\,\frac{\sigma_a}{\bar{\sigma}}. \quad (30)$$

Thus a tensile stress is required. The condition for holes to remain open requires that the eccentricity be less than unity, or, from equation (20), both transverse components of stress must be tensile. Thus from this analysis fracture by hole growth cannot quite occur in the tensile test before necking, in torsion (neglecting the effects of rotation) or in uniaxial compression (open die forging).

Note how difficult it would be to effect any great increase in ductility by increasing the purity. To raise the ductility in the doubly grooved plane-strain specimen by a factor of ten, to $\bar{\epsilon}^f = 0.50$, would require a growth factor of 10^{10}, corresponding to a void fraction of 10^{-30}, or one atomic vacancy in 100 tons of material!

The strong interaction between triaxiality and strain hardening is shown by Fig. 12 or equation (28). Under the low triaxiality of plane strain bending, $(\sigma_a+\sigma_b)/\bar{\sigma} = \sqrt{3}$, increasing the strain-hardening index from $n = 0$ to $n = 0.3$ increases the fracture strain by 20 percent. However, as n is increased from 0 to 0.3 the fracture strain is increased by a factor of 2.8, for the high triaxiality expected in front of a crack, $(\sigma_a+\sigma_b)/\bar{\sigma} = 5.36$ [from the fully plastic solution with $\sigma_a = (1+\pi/2)(2\bar{\sigma}/\sqrt{3})$, $\sigma_b = (1/2+\pi/2)(2\bar{\sigma}/\sqrt{3})$]. This effect, as well as the change in stress distribution itself, is no doubt an important contribution to the effect of strain hardening on fracture toughness reported by Krafft [19]. A quantitative prediction would require at least an approximation to the effect of strain hardening on the relation between fracture strain and stress intensity factor given by

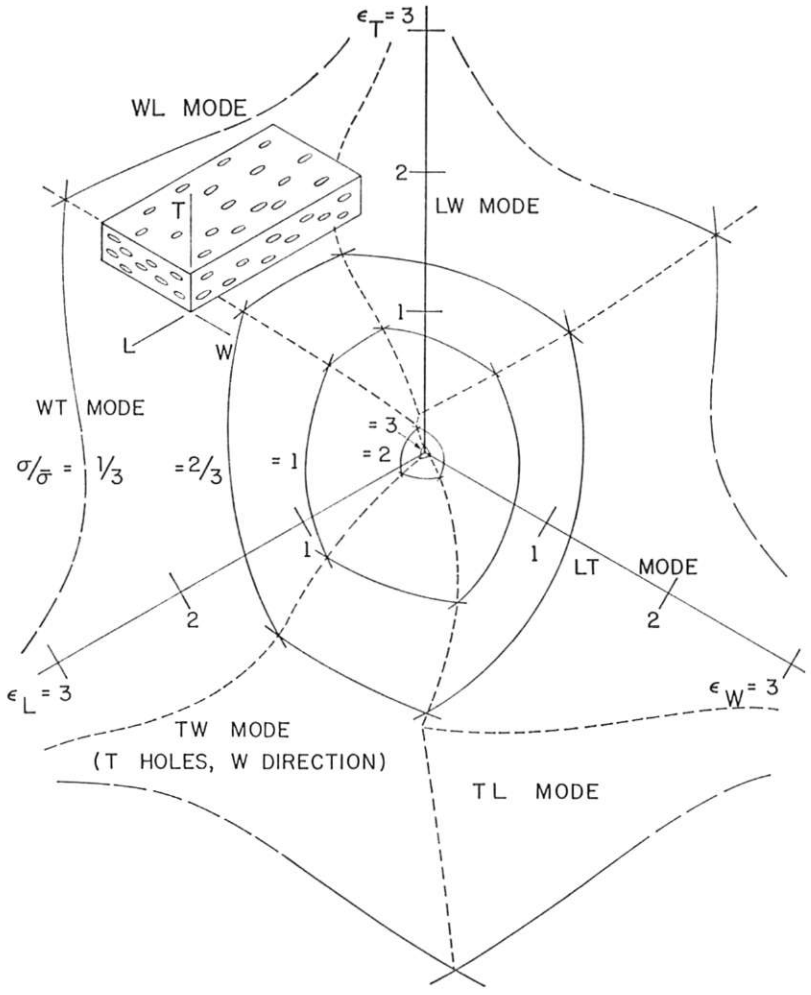

Fig. 13 Dependence of fracture strain on mean normal stress in a rolled slab. Anisotropic hole growth factors of Table I assumed

McClintock's equations (80) and (62) [20].

The effect of size on fracture appears in the need for acquiring the critical strain over a region enclosing two or more inclusions. Thus of two geometrically similar notched specimens of the same material, the larger will fail at the lower applied strain.

Application to a rolled slab. Consider the rolled slab sketched in Fig. 13, for which hypothetical growth factors at fracture are given in Table 1. Note that if the original casting was isotropic

Table 1 Hypothetical growth factors at fracture, F_{ij}^f assumed for Fig. 11

Hole axis → / Growth axis	L	W	T
L	—	60	120
W	30	—	80
T	20	40	—

as regards fracture, and if the distortion of the inclusions during rolling was the same as that of the billet, the ductility would still be isotropic, since the ratio a/l would not change. Note also that for random, as opposed to layered configurations, the growth factors to fracture are not likely to differ too greatly for two different directions of growth from the same hole, since growth need not be confined to strictly orthogonal directions.

The resulting fracture locus for a nonhardening material is shown in Fig. 13 for constant ratios of applied stress. For the lowest mean normal stress, $\sigma = \bar{\sigma}/3$, the strain becomes infinity as one of the transverse stress components goes to zero, due to the closing of the holes. At this normal stress, all six mechanisms of fracture can occur, but at mean normal stress ratios of 2 and 3 only three mechanisms can operate. Again, the most striking result is the very low fracture strain at these high normal stress ratios.

Application to tensile tests. The necking in a tensile test requires that the effect of changing transverse stress can be taken into account. Bridgman [21] found that the ratio of section radius a to profile radius R is,

for

$$\epsilon_z > 0.1,$$

$$\frac{a}{R} = 2.93\,\{1 - \exp\,[-(\epsilon_z - 0.1)/3]\}^{*} \tag{31}$$

If the strain is uniform across the neck, the radial stress is given by

$$\sigma_r/\bar{\sigma} = \ln\,(1 + a/2R). \tag{32}$$

Evaluation of equations (23) and (24) in short steps for this tensile stress-strain history for different modes of fracture and strain-hardening coefficients of $n = 0$ and $n = 1$, using the aforementioned computer program, yields the growth factors shown in Fig. 14.

Tensile tests of a variety of materials by Henry [22] and Alpaugh [23] showed that, except for 1100-0 aluminum, the tensile ductility was only a fraction of that expected for materials of reasonable purity ($F^f \approx 10$). While Bluhm and Morrissey [5] have shown, as did Alpaugh, that fracture in the tensile test begins by relatively homogeneous growth of holes from inclusions, their experiments as well as those of Rogers [4] show that the deformation becomes localized into thin shear bands, after which slight overall deformation is sufficient to cause fracture. Pending an investigation of this instability, one can only say that the homogeneous growth of holes provides an introduction to the instability study and an upper limit to the ductility.

Review of assumptions. The assumption that holes are initially present may be good for weak inclusions or interfaces. In other cases, strain hardening may be required to produce fracture in the more brittle phases of an alloy. Clausing [24] found both cases to be present in the same steel.

The cylindrical holes assumed here might be replaced by

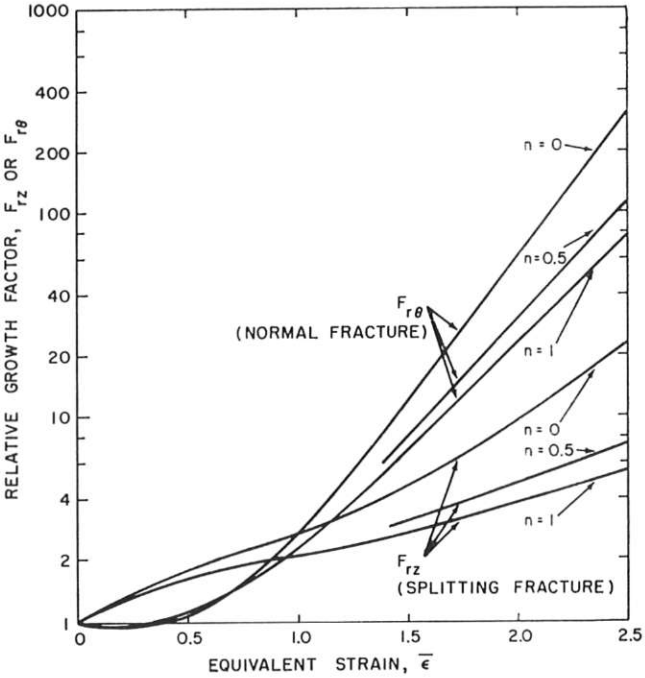

Fig. 14 Relative growth factor in a tensile test

ellipsoidal holes, but experience with other two versus three-dimensional problems suggests that the difference would be small. For instance, for expansion of spherical and cylindrical holes in incompressible materials under pure triaxial tension, Hill [25] reports

$$\sigma/\bar{\sigma} = [1 + \ln\,(E/\sqrt{3}\,\bar{\sigma})]/\sqrt{3},$$

and

$$\sigma/\bar{\sigma} = [1 + \ln\,(E/1.5\bar{\sigma})]/1.5, \tag{33}$$

respectively.

Exact plasticity solutions for hole growth in a deforming medium have been obtained only for circular symmetry and equiaxial transverse stress. But even this case illustrates the strong effect of triaxiality, which is the major result. At low triaxiality, the condition that the holes remain open makes the intermediate principal stress more important, and here more work is required, for the shape of the hole becomes important. When the holes close, further study is required, for although fracture under transverse pressure is not predicted by the theory, it does occur.

While a viscous material does not fracture but rather "strings out," it is used here only to give an approximate relation for a linearly strain-hardening material, which does fracture. For instance, in uniaxial tension, if $d\sigma/d\epsilon = C$, necking begins at a strain of unity.

The rigid-plastic assumption becomes untenable at high triaxiality, for, as equation (33) indicates, the normal stress for fracture under pure triaxial tension drops from the infinite value for a rigid material to 3 to 5 times the equivalent flow stress for $E/\bar{\sigma} = 100$ to 1000.

Conclusions

A quantitative fracture criterion has been developed for fracture by the growth and coalescence of preexisting holes in plastic materials. For varying ratios of principal components of stress the fracture criterion is found by applying equations (23), (24), and (26) to successive short increments of strain, during any one of which the stress ratios are constant. An approximate analytical expression of the criterion is given by equation (28), or for constant stress history by equation (29). This criterion pro-

vides a useful contrast to the Griffith theory for the fracture of brittle materials under combined stress. Presumably, the behavior of materials with limited ductility, or in which nucleation by cracking of inclusions was controlling, would lie somewhat between these extreme theories.

When expressed in terms of strain deviators, the graphical form of presentation of the hole growth criterion would be valid for any other mechanisms of fracture in which the principal components of stress do not rotate, and also for yielding.

The criterion for fracture by hole growth illustrates the following points:

1 The very strong inverse dependence of fracture strain on tensile stress transverse to the holes.

2 The relatively strong dependence of fracture strain on the transverse (intermediate) principal stress, rather than solely on the mean normal stress or the maximum principal stress.

3 The dependence of ductile fracture on the *history* of stress and strain.

4 The need for squaring the initial void fraction in order to double the fracture strain.

5 The anisotropy of fracture which may arise out of an initially anisotropic shape and spacing of the holes.

6 The increase in fracture strain to be expected from increased strain hardening, judging from the viscous as compared to the ideally plastic results.

7 A size effect in fracture, as indicated by the need for attaining critical values of the strain and stress history over a region of the order of the hole spacing before fracture will occur.

8 The fact that other mechanisms also contribute to ductile fracture in most cases, since the strains required for fracture of holes commonly observed in structural metals are rather smaller than found above, considering the low inclusion count and the presence of strain hardening.

9 The need for studying the localization of flow within plastic, slightly porous materials.

Acknowledgment

It is a pleasure to acknowledge the help of V. A. Tipnis and the following undergraduates who took part in developing these ideas and making experiments: Stephen C. Dangel, George H. East, Jr., Roger L. Hybels, and Stephen H. Kaiser. The support of the National Science Foundation, through Grant G-14995, is deeply appreciated.

References

1 Tipper, C. F., "The Fracture of Metals," *Metallurgia*, Vol. 39, 1949, pp. 133–137.

2 Plateau, J., Henry, G., and Crussard, C., "Complements à l'Interpretation des Images Fournies par la Microfractographies," *Metaux, Corrosion Industries*, Vol. 33, 1958, pp. 141–162.

3 Puttick, K. E., "Ductile Fracture in Metals," *Philosophical Magazine*, Series 8, Vol. 4, 1959, pp. 964–969.

4 Rogers, H. C., "Tensile Fracture of Ductile Metals," *Trans. Metallurgical Society of AIME*, Vol. 218, 1960, pp. 498–506.

5 Bluhm, J. I., and Morrissey, R. J., "Fracture in a Tensile Specimen," *Proceedings of First International Conference on Fracture, Sendai*, Japanese Society for Strength and Fracture of Materials, Vol. 3, 1966, pp. 1739–1780.

6 Rhines, W. J., "Ductile Fracture by the Growth of Pores," MS thesis, M.I.T., Department of Mechanical Engineering, 1961.

7 Backofen, W. A., Shaler, A. J., and Hundy, B. B., "Mechanical Anisotropy in Copper," *Trans. ASM*, Vol. 46, 1954, pp. 655–675.

8 Edelson, B. I., "Strain Concentrations and Ductility," *Trans. Quarterly of ASM*, Vol. 56, 1963, pp. 82–89.

9 Gurland, J., and Plateau, J., "The Mechanism of Ductile Rupture of Metals Containing Inclusions," *Trans. Quarterly of ASM*, Vol. 56, 1963, pp. 442–454.

10 Beachem, C. D., "An Electron Fractographic Study of the Influence of Plastic Strain Conditions Upon Ductile Rupture Processes in Metals," *Trans. Quarterly of ASM*, Vol. 56, 1963, pp. 318–326.

11 Bluhm, J. I., and Morrissey, R. J., "Preliminary Investigation of the Fracture Mechanism in a Tensile Specimen," U. S. Army Materials Research Agency, Watertown, Mass., May 1964.

12 McClintock, F. A., Kaplan, S. M., and Berg, C. A., "Ductile Fracture by Hole Growth in Shear Bands," *International Journal of Fracture Mechanics*, Vol. 2, No. 4, 1966, pp. 614–627.

13 Drucker, D. C., "On Obtaining Plane Strain or Plane Stress Conditions in Plasticity," *Proc. Second U. S. National Congress of Applied Mechanics*, ASME, 1954, pp. 485–488.

14 McClintock, F. A., and Rhee, S. S., "On the Effects of Strain Hardening on Strain Concentrations," *Proc. Fourth U. S. National Congress of Applied Mechanics*, ASME, Vol. 2, 1962, pp. 1007–1014.

15 Berg, C. A., "The Motion of Cracks in Plane Viscous Deformation," *Proc. Fourth U. S. National Congress of Applied Mechanics*, ASME, Vol. 2, 1962, pp. 885–892.

16 Hybels, R., "Bulge Tests of Hole Growth in Plasticine," Research Memo. No. 64, Fatigue and Plasticity Lab., M.I.T., Department of Mechanical Engineering, 1963.

17 East, G., personal communication.

18 Moorer, J. A., and McClintock, F. A., "The Fracture Tracker," Research Memo 82R, Fatigue and Plasticity Lab., M.I.T. Department of Mechanical Engineering, December 1966.

19 Krafft, J. M., "Correlation of Plane Strain Crack Toughness With Strain Hardening Characteristics of a Low, a Medium, and a High Strength Steel," *Applied Materials Research*, Vol. 3, April 1964, 88–101.

20 McClintock, F. A., "Effects of Root Radius, Stress, Crack Growth and Rate on Fracture Instability," *Proceedings of the Royal Society*, Series A, Vol. 285, 1965, pp. 58–72.

21 Bridgman, P. W., *Studies in Large Plastic Flow and Fracture*, McGraw-Hill, New York, 1952

22 Henry, M. F., "Investigation of Fine Cracks in Ductile Fracture," MS thesis, M.I.T. Department of Mechanical Engineering, 1966.

23 Alpaugh, H. E., "Investigation of the Mechanisms of Failure in the Ductile Fracture of Mild Steel," BS thesis, M.I.T. Department of Mechanical Engineering, 1965.

24 Clausing, D. P., "The Development of Fibrous Fracture in Mild Steel," *Trans. Quart. ASM*, Vol. 60, No. 3, September 1967, pp. 504–515.

25 Hill, R., *Mathematical Theory of Plasticity*, Oxford, 1950, pp. 104 and 127.